

# Highly Porous Paper Loading with Microfibrillated Cellulose by Spray Coating on Wet Substrates

Davide Beneventi,<sup>\*,†</sup> Didier Chaussy,<sup>†</sup> Denis Curtil,<sup>†</sup> Lorenzo Zolin,<sup>‡</sup> Claudio Gerbaldi,<sup>‡</sup> and Nerino Penazzi<sup>‡</sup>

<sup>†</sup>Grenoble Institute of Technology, UMR 5518 CNRS—Grenoble—INP, Domaine Universitaire, 461 rue de la Papeterie, BP 65, 38402 St. Martin d'Hères, France

<sup>‡</sup>Politecnico di Torino, Department of Applied Science and Technology—DISAT, GAME Lab, Corso Duca degli Abruzzi 24, 10129 Torino, Italy

**ABSTRACT:** A laboratory bench for the spray coating of aqueous slurries on wet substrates and the subsequent water removal by vacuum filtration was used to load porous papers with microfibrillated cellulose (MFC). Spray coating provided an accurate control of the coating basis weight and, when increasing the MFC load, homogeneous films progressively formed on the substrate with negligible loss of MFC. Even in the presence of porous papers, the MFC coating remained confined on the surface of the substrate, at first forming irregular pots and then, as the MFC basis weight exceeded 6 g/m<sup>2</sup>, a continuous film. The formation of a MFC film induced a drop in the air permeability and a sharp increase in the tensile properties. Also, after film formation, the further increase of the MFC coating basis weight led to a linear increase of the tensile properties that, as for laminates, were predicted by the rule of mixtures.

## ■ INTRODUCTION

Since its first introduction by Turbak et al. in 1983,<sup>1</sup> microfibrillated cellulose (MFC) appeared as a biosourced nanomaterial with vast application potential. Nevertheless, the high energy consumption needed to release cellulose micro/nano fibrils from the pristine vegetal fibers strongly limited the interest toward this material which remained disregarded for almost two decades.<sup>2</sup> Lately, the development of new disintegration protocols based on chemical or enzymatic pulp pretreatments allowed decreasing energy consumption, which dropped from ca. 30 MWh/ton to 1–10 MWh/ton,<sup>3–5</sup> depending on the final defibration grade. The availability of viable mass production processes opened the perspective for new industrial applications that, leaving aside both structural and functional nanocomposites,<sup>2,6,7</sup> are mainly focused on the manufacture of all cellulose composite sheets and coatings.<sup>8</sup>

Individual cellulose microfibrils have elastic modulus ranging between 130 and 200 GPa<sup>9,10</sup> and, upon drying, can assemble into dense networks generating bulky films with high modulus, ca. 10–20 GPa, and interesting gas/oil barrier properties.<sup>8,11–14</sup>

In recent studies, aimed at developing all cellulose packaging materials with improved mechanical and barrier properties, MFC was either mixed with wood fibers and used for the production of MFC–wood fiber composite sheets by filtration<sup>15–19</sup> or coated onto the surface of preformed paper to form a bilayer.<sup>12,14,21–23</sup> Both approaches led to the increase of the mechanical and barrier properties the final paper sheet. However, even if requiring an additional unit operation, the coating process leads to the formation of a continuous MFC film that induces a drop of two, up to five, orders of magnitude in the air permeability of the pristine substrate<sup>12,14,22</sup> in contrast with the limited 2–25 fold decrease provided by MFC–wood fiber composite sheets.<sup>15,17,20</sup> Therefore, the coating process appears as the most viable technique for the preparation of

MFC–wood fibers paper sheets with enhanced barrier properties.

In line with a previous study,<sup>24</sup> where a spray coating unit was implemented on the wet end of a pilot paper machine and used to deposit a graphite–MFC film on a forming paper sheet, this work was aimed at demonstrating that MFC spray coating on wet paper substrates can be used for the manufacture of coated papers with high strength and air barrier properties.

## ■ EXPERIMENTAL SECTION

**Materials. Paper Substrates.** Three different papers with increasing apparent density were used as substrate for spray-on-wet coating. Namely, two commercial nonwoven papers supplied by PDM Industries, made of abaca pulp and mixes of abaca and wood pulp (labeled as V1 and V2), and paper hand sheets processed using a 37 °SR bleached softwood (spruce) kraft pulp and a rapid Köthen hand sheet former (labeled as BKP). Main characteristics of the tested substrates obtained during preliminary tests are summarized in Table 1.

**Microfibrillated Cellulose.** MFC used for paper substrates coating was produced by FCBA, Grenoble. A hardwood bleached Kraft pulp was disintegrated in water at 5% consistency for 15 min. Subsequently, a prerefining stage was carried out using a 12" single-disc pilot refiner system on 5 kg of oven-dried pulp. The objective of this first refining stage was to obtain a slightly refined pulp with a drainage index close to 25 °SR. An enzymatic treatment was then applied on the prerefined pulp at 5% consistency with a commercial cellulase, FibreCare R (Novozymes, Denmark), at a concentration of

**Received:** March 5, 2014

**Revised:** June 10, 2014

**Accepted:** June 12, 2014

**Published:** June 12, 2014

Table 1. Main Properties of Paper Substrates Used for Wet Spray Coating<sup>a</sup>

substrate	basis weight (g m <sup>-2</sup> )	thickness (μm)	apparent density (kg m <sup>-3</sup> )	Gurley air permeability (s 100 mL <sup>-1</sup> )	Young's modulus (GPa)	stress at break (MPa)	strain at break (%)
V1	9.6	30 ± 1	316	~0.5	3.4 ± 0.2	26.4 ± 3	2.3 ± 0.2
V2	12.4	35 ± 1	349	~0.5	2.9 ± 0.4	24.2 ± 2	3 ± 0.1
BKP	35	54 ± 2	651	3	5.9 ± 0.3	31.5 ± 3	3.3 ± 0.1

<sup>a</sup>Properties of V1 and V2 were determined after rewetting and drying on a rapid Köthen hand sheet former.

about 1 mL kg<sup>-1</sup>. The pulp was incubated for 1 h at 50 °C. A second refining stage was performed on the enzymatically pretreated pulp at 5% consistency using the same 12" disk refiner as used for the prerefining step. The pretreated pulp was finally diluted at 2% consistency and used for the production of microfibrillated cellulose by means of a homogenizer Ariete NS3075 (GEA NiroSoavi, Italy) working at a maximum flow of about 1000 L h<sup>-1</sup>. Five passes (i.e., one at 1000 bar and four at 1450 bar) were successively performed into the homogenizer to produce the final MFC suspension.

**Experimental Setup for Spray-on-Wet Coating.** Before MFC coating, nonwoven substrates were dipped in water, placed on a sheet-forming fabric and the excess water was removed by vacuum suction on the rapid Köthen hand sheet former. BKP sheets were elaborated by pouring 200 mL of a 5 g L<sup>-1</sup> pulp slurry in the hand sheet former, followed by vacuum dewatering. In order to avoid sheet damage, loose fiber mats with dry solids content ranging between 15 and 20% were not detached from the forming fabric. Subsequently, MFC was spray coated onto wet substrates using an in house assembled spray coater (see Figure 1) constituted of a variable speed conveyor and a commercial high pressure spray system (paint crew, Wagner). According to the operating conditions of the coating bench (Table 2) and the 2% consistency of the MFC slurry used to feed the coater, the basis weight ( $bw_{MFC}$ ) of the

MFC coating, given as the mass of MFC per unit surface of substrate, was affected only by the conveyor speed. It was estimated using the following equation, which was derived from the geometry of the experimental set up

$$bw_{MFC} = \frac{\dot{m} \cdot c}{2D \tan \theta \cdot V} \quad (1)$$

where  $\dot{m}$  and  $c$  are the mass flow and the consistency of the MFC slurry, respectively,  $D$  is the nozzle distance from the substrate,  $V$  is the conveyor speed, and  $\theta$  is the spray jet angle calculated using  $D$  and the width ( $W$ ) of the main jet impact area, where most of the MFC slurry was projected. Satellite droplets that generated a larger impact area were neglected and all the sprayed material was supposed to be homogeneously distributed over the main impact zone.

According to eq 1, the conveyor speed was ranged between 12 and 1 m min<sup>-1</sup> in order to deposit a MFC coating having a (dry solids) basis weight between ca. 3 and 40 g m<sup>-2</sup>. After the deposition of the MFC slurry, the substrate was coated by a glossy MFC gel corresponding to a water film of ca. 150 up to 2000 g m<sup>-2</sup>. The forming fabric-supported substrate was then transferred to the rapid Köthen hand sheet former and the excess water was removed by vacuum suction. Finally, the coated sheet was pressed (3 kg roll) against blotting paper, sandwiched between two coated cardboards, and dried at 80 °C in a vacuum dryer.

A MFC film was also elaborated by spray coating the MFC slurry on a stainless steel plate at a fixed conveyor speed of 5 m min<sup>-1</sup> (corresponding to a deposit of ca. 8 g m<sup>-2</sup> of dry MFC, as calculated by eq 1). The film was air-dried during 1 day at room temperature in order to avoid excessive shrinkage and crackling.

**Sheet Characterization.** In order to quantify the contribution of the MFC coating on sheet topography, uncoated and coated sheets were imaged by an optical microscope (430× magnification) and their surface roughness was measured using an optical 3D profilometer (Infinite Focus, Alicona). The 3D profile was discretized in 4.5 μm width lines and surface roughness,  $R_{RMS}$ , was calculated as the root mean squared of the vertical distance from the mean profile height.  $R_{RMS}$  values are given as the average of ten measurements performed on 1.42 × 1.08 sample areas.

Air permeability, expressed as the time needed by 100 mL of air to flow through the paper sample, as well as sheet thickness were measured using a standard Gurley SPS Tester and a mechanical caliper (Adamel Lhomargy, MI20), respectively. The mechanical properties of the MFC film and the coated sheets were evaluated by (i) traction tests (Instron, 5969) on 5 × 1.5 cm strips with a strain rate of 5 mm min<sup>-1</sup> and (ii) internal bond strength (Scott Bond, IDM test IBT-10A) according to the Tappi T569 standard. All mechanical properties are provided as the average of five replicates.

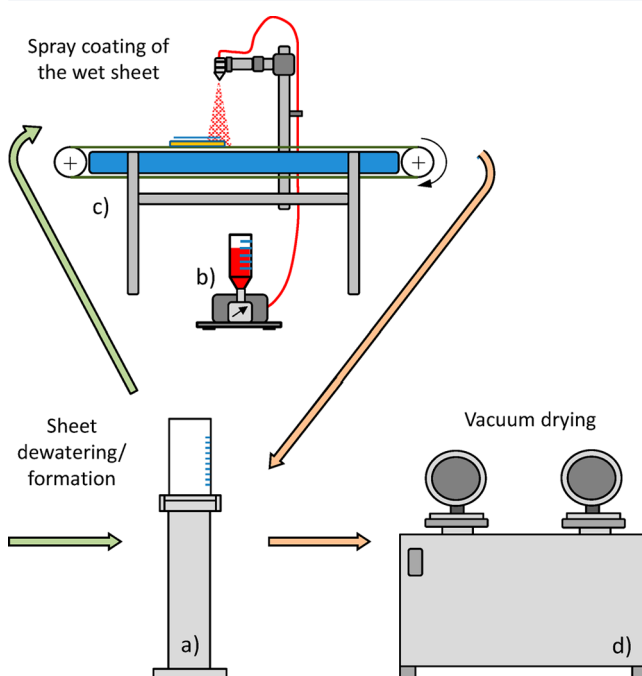


**Figure 1.** Scheme of both the coating bench and the experimental procedure used for MFC wet coating of paper substrates. (a) Rapid Köthen hand sheet former, (b) high pressure spray system, (c) variable speed conveyor, and (d) rapid Köthen vacuum dryer.

Table 2. Operating Conditions of the Spray Coating Bench Developed in This Study<sup>a</sup>

conveyor speed (m min <sup>-1</sup> )	spray pressure (bar)	spray flow (g min <sup>-1</sup> )	nozzle area (mm <sup>2</sup> )	nozzle ellipticity $d_{\max}/d_{\min}$	spray jet angle (deg)	nozzle-conveyor distance (m)	spray jet width (m)
0.5–12	190	750	0.28	2.1	56	0.36	0.38

<sup>a</sup> $d_{\max}$  and  $d_{\min}$  are the nozzle major and minor axis, respectively.

## RESULTS AND DISCUSSION

Spray coating of the MFC slurry on a smooth stainless steel plate led to the formation of a 6  $\mu\text{m}$  thick MFC film displaying a pinhole-free surface and an apparent density of  $1260 \pm 200 \text{ kg m}^{-3}$ , close to that of MFC films formed by pressure molding<sup>23</sup> and vacuum filtration,<sup>11</sup> that is, 1480 and  $1340 \text{ kg m}^{-3}$ , respectively. However, the film structure, apparently homogeneous at the micrometric scale, was accompanied by an extremely brittle behavior and, as illustrated in Figure 2, film

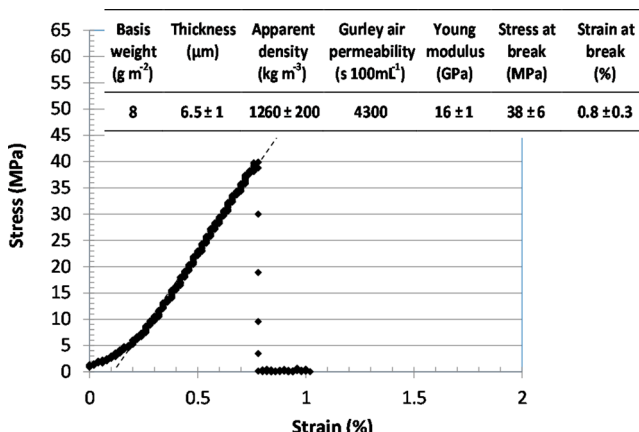


Figure 2. Typical stress strain curve of the bare MFC film. The table in the inset lists the relevant film properties. MFC air permeability was reported for qualitative comparison with MFC coated papers; please note that above 1800 s, air leakage can affect measurement reliability.

fracture occurred in the elastic deformation domain. Thereafter, a Young's modulus of  $16 \pm 1 \text{ GPa}$ , in line with the elasticity currently obtained for MFC films,<sup>11–13</sup> was accompanied by stress and strain at break of  $38 \pm 6 \text{ MPa}$  and  $0.8 \pm 0.3\%$ , respectively. These values (3 to 10 folds lower than the ca. 110–130 MPa and 5–8% determined for 25–90  $\mu\text{m}$  thick films,<sup>11–13</sup> respectively) were ascribed to the presence ca. 1  $\mu\text{m}$  diameter  $\times$  80  $\mu\text{m}$  length fiber debris in the MFC slurry used in this study<sup>5</sup> and to flaws (i.e., fracture nucleation spots) they can generate in thin MFC film.

Figure 3 shows that all MFC coated papers had basis weight close to that calculated using eq 1 and the basis weight of the uncoated substrates. This trend demonstrated the good repeatability of the spray coating procedure and, in line with previous works,<sup>12,23,26</sup> the complete retention of MFC on the wet substrate during the dewatering stage by vacuum filtration. MFC retention on wet substrates having highly porous structure and ca. 250, 200, and 80  $\mu\text{m}$  open pores (as estimated from Figure 4) for V1, V2, and BKP, respectively, was associated with the high MFC concentration in the coating slurry (i.e., 2%) and the ensuing formation of a densely packed percolation network, which immobilized individual nanofibrils in a macro flock.<sup>23</sup>

After spray coating, MFC formed a homogeneous liquid film. However, Figure 4 illustrates that when using the lowest basis weight of deposited MFC (3 g m<sup>-2</sup>), MFC film shrinkage upon

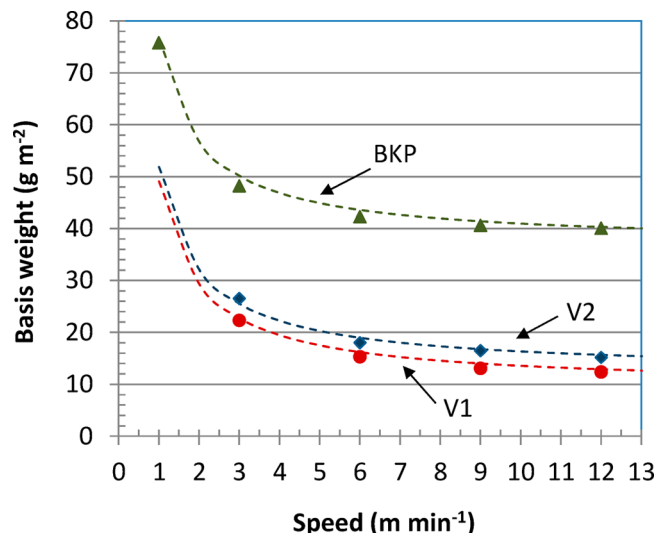


Figure 3. Basis weight of the paper substrates coated at different conveyor speed. Dashed lines represent the substrates' basis weight calculated by adding the basis weight of the MFC coating given by eq 1 to the basis weight of the uncoated substrates.

drying and the high porosity of the V1 and V2 substrates (i.e., 79 and 77%, respectively) led to a partial coverage of the paper substrate.

It is noteworthy that a quite homogeneous film formed by depositing 4 g m<sup>-2</sup> of MFC on both the low porosity (57%) BKP sheet and on the V1 and V2 substrates where the increase of MFC basis weight, from 3 to 4 g m<sup>-2</sup>, led to pores clogging and at 6 g m<sup>-2</sup> a continuous MFC film formed (see Figure 4).

Under the hypothesis of a negligible penetration of the MFC slurry in the substrate and the formation of a homogeneous film, the thickness ( $e$ ) and the density ( $\rho$ ) of the coated sheets were calculated as

$$e = e_s + \frac{bw_{\text{MFC}}}{\rho_{\text{MFC}}} \quad (2)$$

and

$$\rho = \frac{bw_s \cdot bw_{\text{MFC}}}{e} \quad (3)$$

where  $e_s$  is the thickness of the uncoated substrate,  $bw_{\text{MFC}}$  and  $bw_s$  are the basis weight of the MFC coating and the uncoated substrate, respectively, and  $\rho_{\text{MFC}}$  is the apparent density of the bare MFC film (i.e.,  $1260 \text{ kg m}^{-3}$ ).

Figure 5 shows that the coated substrate thickness and the apparent density linearly increased with the basis weight of the MFC coating.

Moreover, both thickness and density values calculated with eqs 2 and 3 reasonably matched with the experimental data, thus supporting the hypothesis of the formation of a MFC coating on the surface of the substrate. Nevertheless, both optical microscopy images (Figure 4) and air permeability data presented in Figure 6 show that pores coverage occurred for a

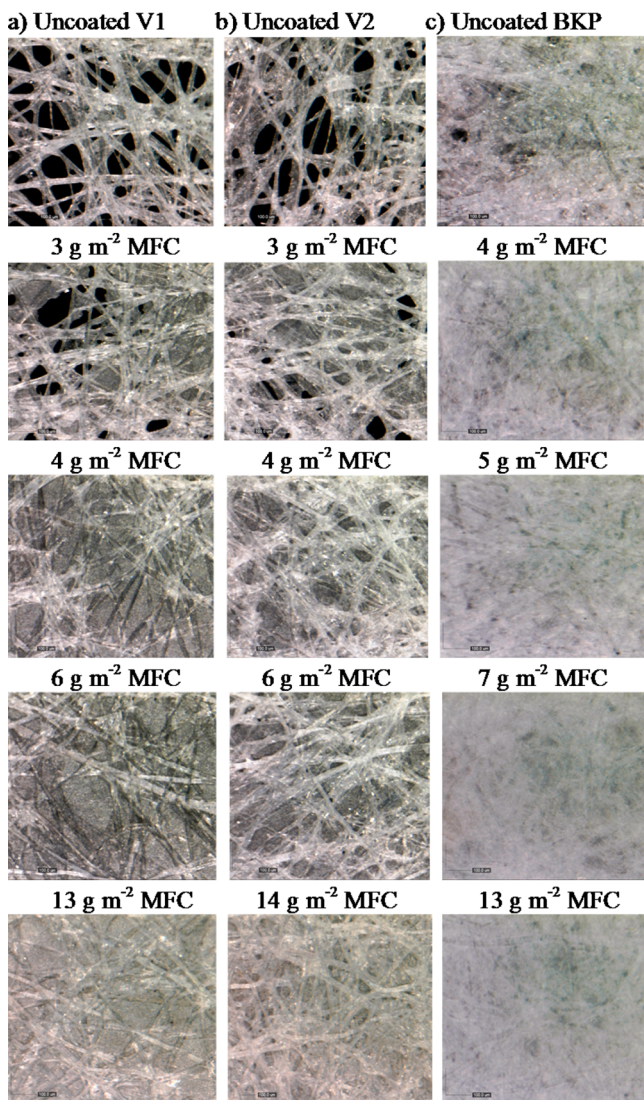


**Figure 4.** Optical microscopy images ( $430\times$ ) of both uncoated and coated substrates. (a) Substrate V1, (b) substrate V2, and (c) BKP substrate.

MFC basis weight higher than  $4\text{--}5\text{ g m}^{-2}$ , when the Gurley air permeability abruptly increased until leveling off above  $6\text{ g m}^{-2}$ .

The hypothesis of the formation of a homogeneous MFC coating was therefore considered valid for a deposited MFC basis weight higher than  $4\text{--}5\text{ g m}^{-2}$ . The surface topography of BKP was slightly modified by increasing the thickness of the MFC coating. Indeed, Figure 7 shows that surface roughness decreased from  $1.5$  to  $1.1\text{ }\mu\text{m}$  when the MFC coating basis weight was raised from  $4$  to  $40\text{ g m}^{-2}$ .

Thick ( $10\text{--}24\text{ }\mu\text{m}$ ) MFC coatings covered the  $2\text{--}4\text{ }\mu\text{m}$  deep  $\times$   $50\text{ }\mu\text{m}$  width short-range irregularities of the pristine BKP substrate; the contour of cellulose fibers progressively faded until disappearing for a MFC film thickness of  $24\text{ }\mu\text{m}$ . However,  $8\text{ }\mu\text{m}$  deep  $\times$   $150\text{--}200\text{ }\mu\text{m}$  width long-range irregularities were partially smoothed by the MFC film; they were also present in the heavyweight coated substrate thus negatively affecting the average film roughness. Such a behavior was ascribed to (i) the homogeneous distribution of the MFC slurry over the paper substrate achieved by the spray coating technique and (ii) its limited ability to fill large pores such as bar or blade coating techniques.<sup>27</sup>

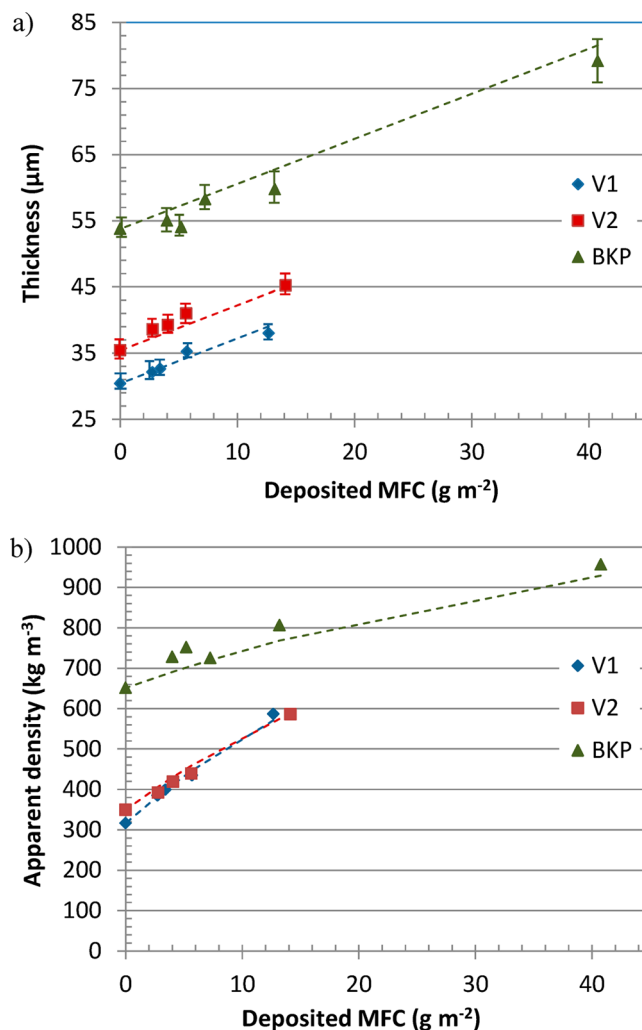


**Figure 5.** Thickness (a) and apparent density (b) of the coated substrates plotted as a function of the MFC coating basis weight. Dashed lines represent data calculated using eqs 2 and 3.

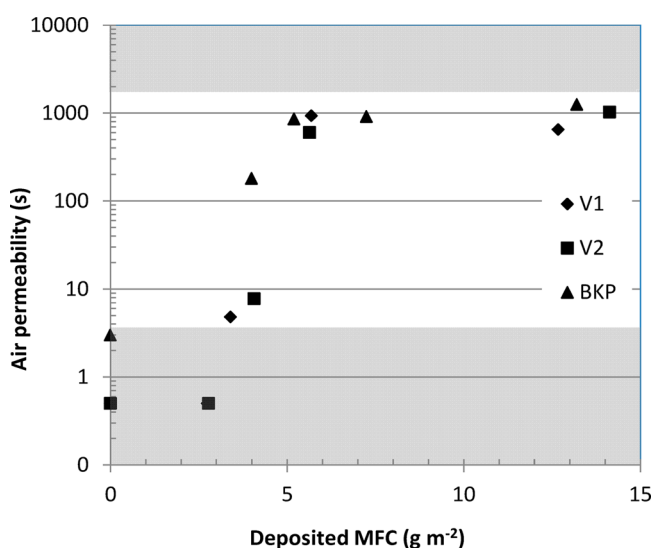


**Figure 6.** Gurley air permeability of MFC coated substrates. Gray areas are out of the recommended measurement range of the Gurley apparatus; data can be affected by low reliability.

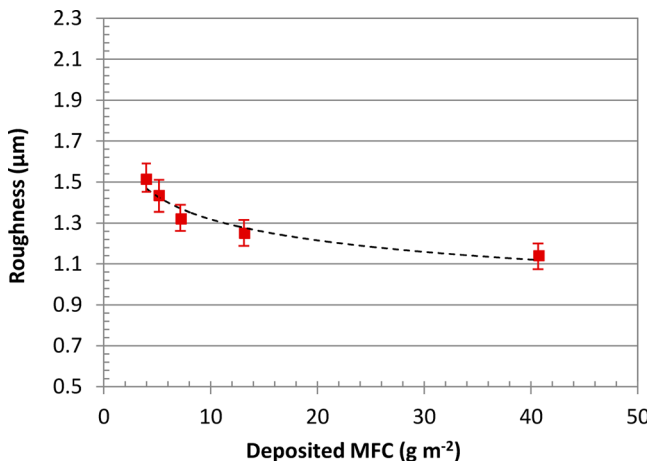


Figure 7. Root mean square roughness of the MFC coated BKP substrate.

For all the tested substrates, the initial formation of an irregular MFC film was accompanied by an abrupt increase of the mechanical properties (Figure 8). Then, as the MFC film became more homogeneous and thick, a progressive shift from a slightly plastic to a brittle behavior was observed (as reflected by the simultaneous increase of the stress at break and the drop of the strain at break).

This trend was even more pronounced when considering the behavior in the elastic deformation domain. Indeed, the plot of the elastic modulus as a function of the MFC film basis weight (Figure 9a) shows a discontinuous behavior where an initial sharp increase of elasticity for low MFC basis weight (i.e., 3–5 g m<sup>-2</sup>) was followed by a linear increase. This might be fitted with the following equation derived from the rule of mixtures<sup>28</sup> and providing the Young's modulus of laminates

$$E = \frac{(E_s e_s + E_{MFC} b w_{MFC}) / \rho_{MFC}}{e} + E_s \alpha \quad (4)$$

where  $E_s$  and  $E_{MFC}$  represent the Young's modulus of the uncoated substrate and the bare MFC film ( $E_{MFC} = 16$  GPa), respectively, and  $\alpha$  represents the initial abrupt modulus increase (expressed as a fraction of the uncoated substrate modulus) for low MFC coating basis weight. Under the tested conditions,  $\alpha$  decreased from 1.1 to 0.3 when  $E_s$  approached  $E_{MFC}$ .

The initial strong elasticity increase was associated with the formation of irregular MFC spots on the substrate (as determined by means of optical microscopy and air permeability, see Figures 4 and 6). Residual large pores were still present, thereafter, the reinforcing action of MFC was supposed to be due to the formation of MFC clusters around fiber contact nodes in the paper substrate and to the increase of interfiber bonding. The following linear increase of the Young's modulus for a basis weight of the MFC coating higher than 5 g m<sup>-2</sup> was in line with the formation of a continuous film. Moreover, the sheet elasticity progressively converged to the modulus of the bare MFC film for all tested substrates.

A similar trend was observed for the stress at break ( $S$ ) of the coated substrates (Figure 9.b); as for the elastic modulus, it was fitted by the following equation<sup>28</sup>

$$S = \frac{S_s e_s + S_{MFC}^{bw_{MFC}/\rho_{MFC}}}{e} + S_s \beta \quad (5)$$

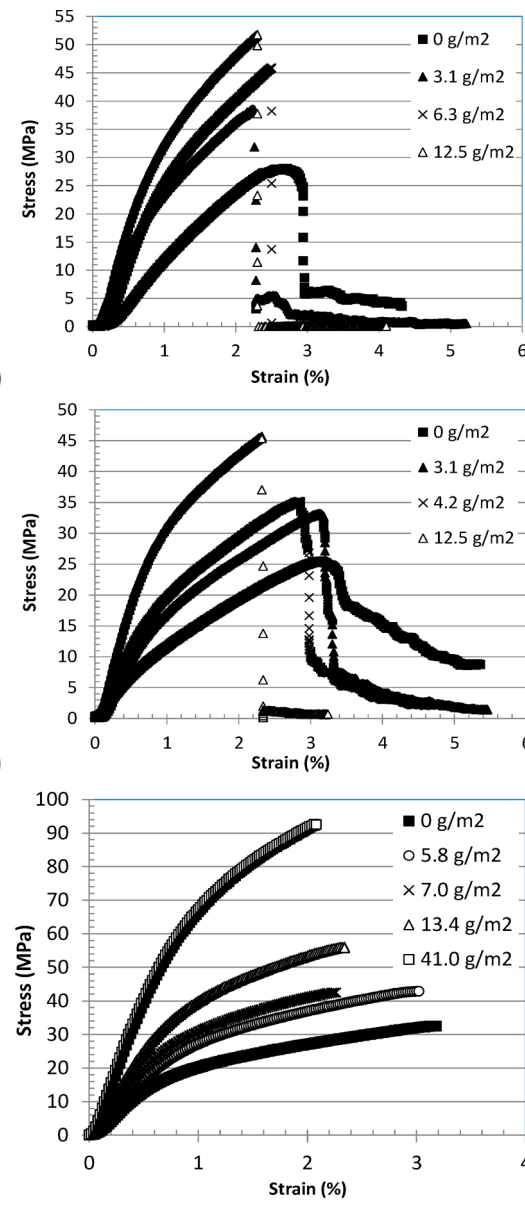
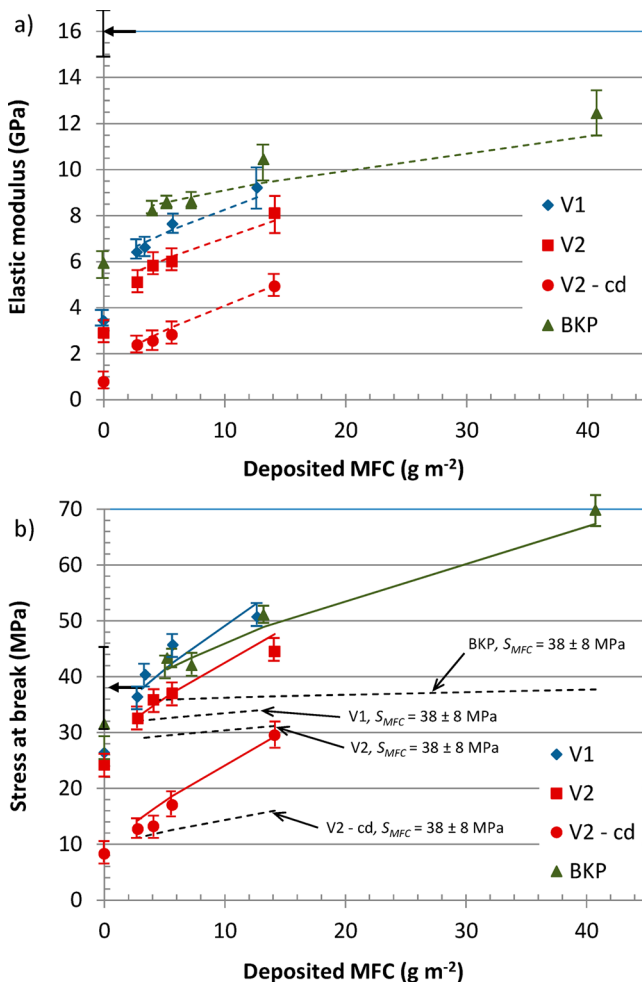


Figure 8. Stress vs strain curves of MFC coated paper substrates (a) V1, (b) V2 and (c) BKP. V1 and V2 stress vs strain curves are representative for the sheet machine direction.

where  $S_s$  and  $S_{MFC}$  are the stress at break of the uncoated substrate and the bare MFC film, respectively, and  $\beta$  represents the initial stress increase (expressed as a fraction of the stress at break of the uncoated substrate) with MFC coatings having low basis weight. For all the tested conditions,  $\beta$  was equal to  $0.16 \pm 0.03$ .

The use of the stress at break of the bare MFC film in eq 5 (i.e.,  $S_{MFC} = 38 \pm 8$  MPa) provided values lower than experimental data. However, when using  $S_{MFC}$  as fitting parameter, a value of  $112 \pm 10$  MPa was obtained, in line with data given in the literature for self-standing MFC films.<sup>11–13</sup> Such a mismatch confirmed that the tensile properties of the thin MFC film obtained by spray deposition on a smooth stainless steel surface were impaired by flaws in the film structure. As a result, this led to the unexpected assumption that the deposition of the MFC slurry on porous cellulosic substrates promoted the formation of tough MFC



**Figure 9.** Mechanical properties of the coated substrates plotted as a function of the MFC coating basis weight. Arrows represent the elastic modulus and stress at break of the bare MFC film. (a) Elastic modulus. Dashed lines represent the elastic modulus given by eq 4. (b) Stress at break of the coated substrates (V2-cd represents the sheet cross direction). Dashed and full lines represent the stress at break obtained with eq 5 when forcing the stress at break of the MFC layer to the value measured for the bare MFC film (i.e.,  $S_{MFC} = 38 \pm 8$  MPa) or when using it as fitting parameter, respectively.

films. Moreover, Figure 9b shows that when they are coated by a MFC basis weight exceeding  $6\text{ g m}^{-2}$ , all substrates had a stress at break higher than that of the bare MFC film, thus indicating the presence of a strong synergy between the MFC film and the substrate.

Figure 10 shows that the internal bond of pristine substrates progressively decreased as their composition was varied from abaca fibers, V1, and abaca/wood pulp mix, V2 (both substrates had a Scott Bond higher than the maximum energy detectable with the testing device) to wood pulp, BKP, which with a Scott Bond of  $315\text{ J m}^{-2}$  displayed the lowest internal bond strength.<sup>29</sup> This trend was in line with the presence of short fibers that, leaving aside the contribution of fiber chemical composition, lead to a general decrease of sheet internal bond strength, owing to the onset of fiber pull out during delamination. As expected, the Scott Bond of the bare MFC film had an extremely high value which was outside the measurement range of the testing device.

For all substrates, the MFC coating induced a progressive decrease of the internal bond strength, which attained a plateau

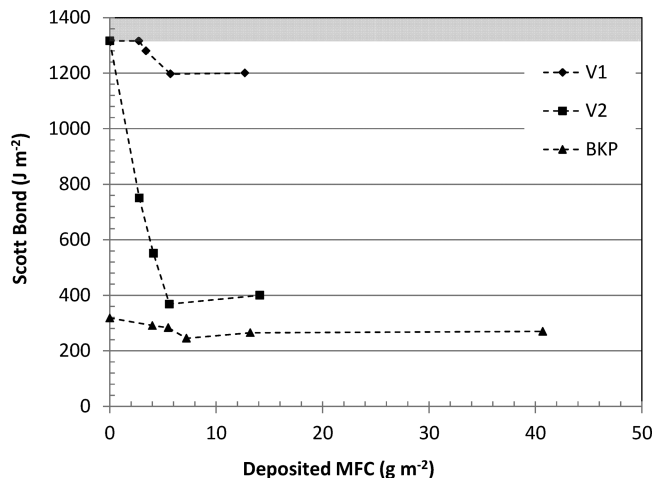


**Figure 10.** Internal bond strength (Scott Bond) plotted as a function of the MFC coating basis weight. The gray area represents the maximum bond energy detectable by the Scott Bond tester.

above  $6\text{ g m}^{-2}$  of deposited MFC. As already assumed for air permeability and tensile properties, this trend was interpreted as reflecting the formation of a continuous MFC film and of a substrate/coating interface whose bond strength was provided by the Scott Bond value at the plateau.

MFC/substrate interfaces on V1, V2, and BKP samples had bond energies of  $1198$ ,  $384$ , and  $260\text{ J m}^{-2}$ , respectively. Abaca fibers were therefore supposed to promote the formation of a tough interface with MFC tightly bound to long fibers that were subjected to limited pull out during delamination. Sample failure occurred via fiber/MFC rupture. In V2 and BKP, the drop in the Scott Bond and the presence of fiber debris on the delamination surface were associated with the presence of short wood fibers and to fiber pull out during delamination.

Overall, Scott Bond measurements confirmed the formation of a continuous coating above  $6\text{ g m}^{-2}$  of deposited MFC.

Experimental data allowed identifying two MFC film formation regimes, that is, film assembly and film thickening, that affected the physical properties of the coated substrate. General trends drawn from this work are summarized in Figure 11.

## CONCLUSIONS

The results reported in this work demonstrate that spray coating of MFC slurries on wet highly porous papers allows obtaining the complete retention of MFC on the surface of the substrate along with a negligible MFC loss during the dewatering stage.

MFC coatings having basis weight up to  $4\text{ g m}^{-2}$  had an irregular structure that resulted in (i) a progressive clogging of the substrate pores and a drop in the permeability to air and (ii) a general sharp increase of ca.  $2.5 \pm 0.5$  GPa and  $9.5 \pm 1$  MPa in the Young's modulus and stress at break, respectively, which was associated with an improved interfiber bonding by MFC clusters.

Above  $6\text{ g m}^{-2}$ , the MFC coating formed a homogeneous film. Air permeability (as detected by the Gurley test) slowly decreased with values of ca.  $1000\text{ s}$  and, in line with the values predicted by the rule of mixtures, the Young's modulus and the stress at break of the coated substrates linearly increased with the increase of the MFC basis weight.

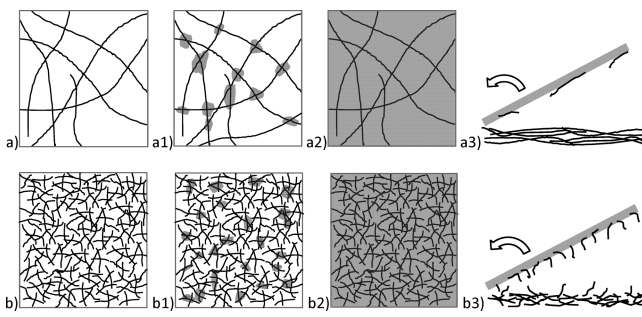


**Figure 11.** Schematic representation of MFC coating on (a) highly porous long fiber substrate and (b) short wood fiber substrate. (a1) and (b1) MFC film assembly with the formation of MFC spots around contact nodes of the fiber substrate. Increase of interfiber bonding and drop of air permeability. (a2) and (b2) Formation and thickening of a continuous MFC film, slight increase of tensile properties and resistance to air permeation. (a3) MFC film delamination by both fiber and fiber/MFC contact areas rupture in the long abaca fiber substrate. (b3) Film delamination by fiber pull out in the short wood fiber substrate.

The composition of the paper substrate strongly affected the bond strength of the MFC coating. Long abaca fiber promoted the formation of a  $1198 \text{ J m}^{-2}$  tough interface whose delamination was ascribed to the rupture of both abaca fiber and of MFC/fiber contact areas. Short fiber induced interface delamination by fiber pull out with a subsequent drop to 384 and  $260 \text{ J m}^{-2}$  of the interface bond strength.

Overall, the experimental results obtained show that the spray coating of MFC slurry on a wet paper substrate may represent a quick and simple technique to improve both air barrier and mechanical properties of paper sheets.

## AUTHOR INFORMATION

### Corresponding Author

\*E-mail: davide.beneventi@pagora.grenoble-inp.fr. Tel.: +33 4 76 82 69 54. Fax: +33 4 76 82 69 33.

### Author Contributions

The manuscript was written through contributions of all authors. All authors have given approval to the final version of the manuscript.

### Notes

The authors declare no competing financial interest.

## ACKNOWLEDGMENTS

Authors wish to thank Mr. Mikael Party for taking surface topography measurements and Mr. Stephane Derrien (PDM Industries) for supplying V1 and V2 paper samples. This work was partially supported by Grenoble Alpes Innovation and Incubation (Gravit, Papel project).

## REFERENCES

- (1) Turbak, A.; Snyder, F.; Sandberg, K. Microfibrillated cellulose, a new cellulose product: properties uses and commercial potential. *J. Appl. Polym. Sci. Appl. Polym. Symp.* 1983, 37, 815–827.
- (2) Siro, I.; Plackett, D. Microfibrillated cellulose and new nanocomposite materials: a review. *Cellulose* 2010, 17, 459–494.
- (3) Ankerfors, M.; Lindström, T. On the manufacture and uses of nanocellulose. *Proc. of 9th Int. Conf. Wood Biofiber Plast. Compos.*; Forest Products Society: Madison, WI, 2007.
- (4) Pääkkö, M.; Ankerfors, M.; Kosonen, H.; Nykanen, A.; Ahola, S.; Osterberg, M.; Ruokolainen, J.; Laine, J.; Larsson, μP.T.; Ikkala, O.; Lindström, T. Enzymatic hydrolysis combined with mechanical shearing and high-pressure homogenization for nanoscale cellulose fibrils and strong gels. *Biomacromolecules* 2007, 8, 1934–1941.
- (5) Meyer, V.; Tapin-Lingua, S.; Da Silva Perez, D.; Arndt, T.; Kautto, J. Technical opportunities and economic challenges to produce nanofibrillated cellulose in pilot scale: NFC delivery for applications in demonstrations trials. *Proc. of SUNPAP EU Project, Final Conference*; VTT Technical Research Centre of Finland: Milan, Italy, 2012; <http://sунpap.vtt.fi/finalconference2012.htm>.
- (6) Eichhorn, S. J.; Dufresne, A.; Aranguren, M.; Marcovich, N. E.; Capadona, J. R.; Rowan, S. J.; Weder, C.; Thielemans, W.; Roman, M.; Rennecker, S.; Gindl, W.; Veigel, S.; Keckes, J.; Yano, H.; Abe, K.; Nogi, M.; Nakagaito, A. N.; Mangalam, A.; Simonsen, J.; Benight, A. S.; Bismarck, A.; Berglund, L. A.; Peijs, T. Review: current international research into cellulose nanofibres and nanocomposites. *J. Mater. Sci.* 2010, 45, 1–33.
- (7) Chuanwei Miao, C.; Hamad, W. Y. Cellulose reinforced polymer composites and nanocomposites: a critical review. *Cellulose* 2013, 20, 2221–2262.
- (8) Lavoine, N.; Desloges, N.; Dufresne, A.; Bras, J. Microfibrillated cellulose – Its barrier properties and applications in cellulosic materials: a review. *Carbohydr. Polym.* 2012, 90, 735–764.
- (9) Iwamoto, S.; Kai, W.; Isogai, A.; Iwata, T. Elastic modulus of single cellulose microfibrils from tunicate measured by atomic force microscopy. *Biomacromolecules* 2009, 10, 2571–2576.
- (10) Nishiyama, Y. Structure and properties of the cellulose microfibril. *J. Wood Sci.* 2009, 55, 241–249.
- (11) Henriksson, M.; Berglund, L. A. Structure and properties of cellulose nanocomposite films containing melamine formaldehyde. *J. Appl. Polym. Sci.* 2007, 106, 2817–2824.
- (12) Syverud, K.; Stenius, P. Strength and barrier properties of MFC films. *Cellulose* 2009, 16, 75–85.
- (13) Henriksson, M.; Berglund, L. A.; Isakson, P.; Lindström, T.; Nishino, T. Cellulose nanopaper structures of high toughness. *Biomacromolecules* 2008, 9, 1579–1585.
- (14) Aulin, C.; Gållested, M.; Lindström, T. Oxygen and oil barrier properties of microfibrillated cellulose films and coatings. *Cellulose* 2010, 17, 559–575.
- (15) Missoum, K.; Martoia, F.; Belgacem, M. N.; Bras, J. Effect of chemically modified microfibrillated cellulose addition on the properties of fiber-based materials. *Ind. Crops Prod.* 2013, 48, 98–105.
- (16) Zhang, L.; Batchelor, W.; Varanasi, S.; Tsuzuki, T.; Wang, X. Effect of cellulose nanofiber dimensions on sheet forming through filtration. *Cellulose* 2012, 19, 561–574.
- (17) Gonzalez, I.; Boufi, S.; Pelach, M. A.; Alcalá, M.; Vilaseca, F.; Mutjé, P. Nanofibrillated cellulose as paper additive in eucalyptus pulps. *Biores.* 2012, 7, 5167–5180.
- (18) Hii, C.; Gregersen, Ø.W.; Chinga-Carrasco, G.; Eriksen, Ø. The effect of MFC on the processability and paper properties of TMP and GCC based sheets. *Nord. Pulp Paper Res. J.* 2012, 27, 388–396.
- (19) Su, J.; Wade, K.; Mosse, J.; Sharman, S.; Batchelor, W. J.; Garnier, G. Effect of tethered and free microfibrillated cellulose (MFC) on the properties of paper composites. *Cellulose* 2013, 20, 1925–1935.
- (20) Taipale, T.; Östertberg, M.; Nykänen, A.; Ruokolainen, J.; Laine, J. Effect of microfibrillated cellulose and fines on the drainage of kraft pulp suspension and paper strength. *Cellulose* 2010, 17, 1005–1020.
- (21) Aulin, C.; Ström, G. Multilayered alkyd resin/nanocellulose coatings for use in renewable packaging solutions with a high level of moisture resistance. *Ind. Eng. Chem. Res.* 2013, 52, 2582–2589.
- (22) Hult, E.; Iotti, M.; Lenes, M. Efficient approach to high barrier packaging using microfibrillated cellulose and shellac. *Cellulose* 2010, 17, 575–586.
- (23) Eriksen, Ø.; Gregersen, Ø.W.; Syverud, K. The effect of MFC on handsheet surface and printing properties. *Proc. of Prog. Paper Phys. Seminar*; Helsinki University of Technology: Espoo, Finland, 2008.
- (24) Beneventi, D.; Chaussy, D.; Curti, D.; Zolin, L.; Bruno, E.; Bongiovanni, R.; Destro, M.; Gerbaldi, C.; Penazzi, N.; Tapin-Lingua, S. Pilot-scale elaboration of graphite/microfibrillated cellulose anodes

for Li-ion batteries by spray deposition on a forming paper sheet. *Chem. Eng. J.* **2014**, *243*, 372–379.

(25) Yano, H.; Nakahara, S. Bio-composites produced from plant microfiber bundles with a nanometer unit web-like network. *J. Mater. Sci.* **2004**, *39*, 1635–1638.

(26) Varanasi, S.; Batchelor, W. J. 2013. Rapid preparation of cellulose nanofibre sheet. *Cellulose* **2013**, *20*, 211–215.

(27) Husband, J. C.; Hiorns, A. G. The Trend towards Low Impact Coating of Paper and Board. *6th Eur. Coating Symp. Proc.*; Bradford, U. K., 2005.

(28) Li, Y. R.; Jiang, H. B.; Cheng, Z. Q. Calculations of the elastic modulus and internal stresses of orthogonal symmetric laminated plates. *Appl. Mech. Mater.* **2013**, *351–352*, 191–194.

(29) Koubaa, A.; Koran, Z. Measure of the internal bond strength of paper/board. *Tappi J.* **1995**, *78*, 103–111.